

Creep behavior of short fiber reinforced composites: Effects of fiber orientation and fiber matrix adhesion

B. Möglinger^a and B. Hausnerova^b

^a*Hochschule Bonn-Rhein-Sieg, von Liebig Str. 20, 53359 Rheinbach, Germany,
bernhard.moeginger@h-brs.de*

^b*Tomas Bata University in Zlín, Faculty of Technology, Department of Production Engineering,
Vavrečkova 275, 762 72 Zlín, Czech Republic
hausnerova@ft.utb.cz*

Abstract. Two grades of 30 weight% short fiber reinforced polypropylene were processed by conventional injection moulding (skin core fiber orientation) and push pull technology (high and uniform fiber orientation in flow direction) to plates. Samples were taken out to determine fiber orientation, mean fiber length, static mechanical properties as well as creep-compliance curves parallel and perpendicular to the flow direction. The creep compliances parallel and perpendicular to the flow direction were modeled using the elementary volume concept (EVC) which assumes that a single elementary volume consisting of a matrix part and a composite part can be used to reproduce the mechanical performance of a short fiber composite. The EVC predicts that the time dependent creep of a short fiber composite depends only on the creep of the pure polymer matrix, fiber volume content, aspect ratio and stiffness of both matrix and fiber. The creep compliance parallel to the flow direction is significantly smaller than perpendicular to it. The measured creep behavior is well reproduced by calculated creep compliances derived by the EVC for the first 2 decades but for longer times experimental data are overestimated. Obviously the presence of fibers generates boundary conditions which change the creep kinetics of the matrix part. The calculated creep curves perpendicular to the flow direction are systematically smaller than the measured curves. However, this can be overcome by the introduction of an adhesion factor which reduces the reinforcement efficiency of the composite part, thus accounting for different fiber matrix adhesions.

Keywords: fiber reinforced polypropylene, creep behavior, fiber orientation, fiber matrix adhesion, modeling of creep, elementary volume concept, adhesion factor

1. INTRODUCTION

In order to improve the mechanical performance of thermoplastic polymers they are often reinforced with short fibers mainly glass or carbon fibers. Parts made of such Short Fiber Reinforced Composites (SFRC) are usually manufactured using injection molding. Due to the complex part geometries the fiber orientation within parts strongly depends on the local flow conditions during mold filling. This leads to the so-called “skin core structure” with preferential fiber orientations parallel to melt flow close to the cavity walls and rather perpendicular in the part center [1]. This not uniform fiber orientation within parts is responsible for anisotropic materials properties and warpage. Therefore, already in the 1960s it was tried to model the mechanical properties of SFRC. The focus laid on determining the components of the stiffness tensor. Three important models can be distinguished:

- The HALPIN-TSAI-model [2] is a generalization of the mixture rule taking into account the mean fiber length, fiber orientation and fiber matrix adhesion in the reinforcement factor ξ .
- The TANDON-WENG-model [3] transfers Eshelby’s treatment of a spherical inclusion [4] to elliptic inclusions.

- The Elementary-Volume-Concept (EVC) [5] which determines the ultimate properties of a unidirectional SFRC consisting of fibers having the same length, **Figure 1**. The fiber orientation of the SFRC is introduced by transformation of the ultimate stiffness tensor with the corresponding orientation tensor [5].

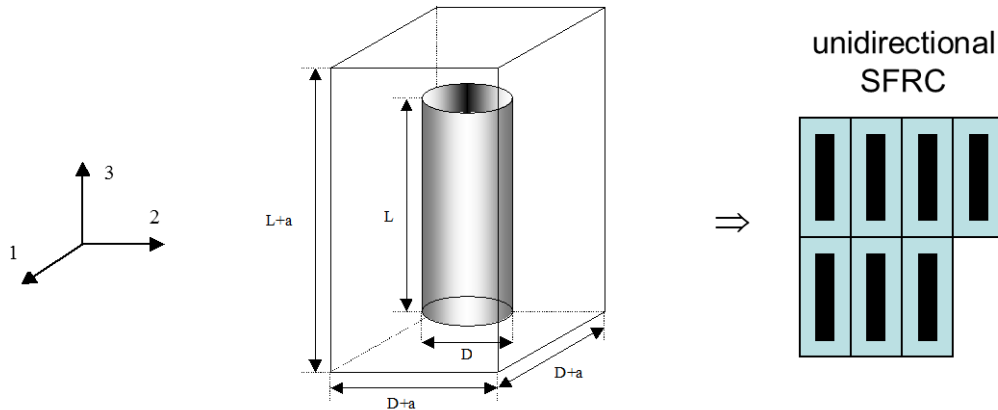


FIGURE 1: Principle of Elementary Volume Concept (EVC) and demonstration of space filling with fiber length L , fiber diameter D and fiber-fiber distance a

Within the EVC the components of the stiffness tensor are derived by dividing the Elementary Volume (EV) in a matrix part and a composite. Then the deformation behavior is considered if an external load is applied on the EV. Due to **Figure 2** it is obvious that matrix part and composite part experience different deformations if the external load acts parallel or perpendicular to the fiber axis.

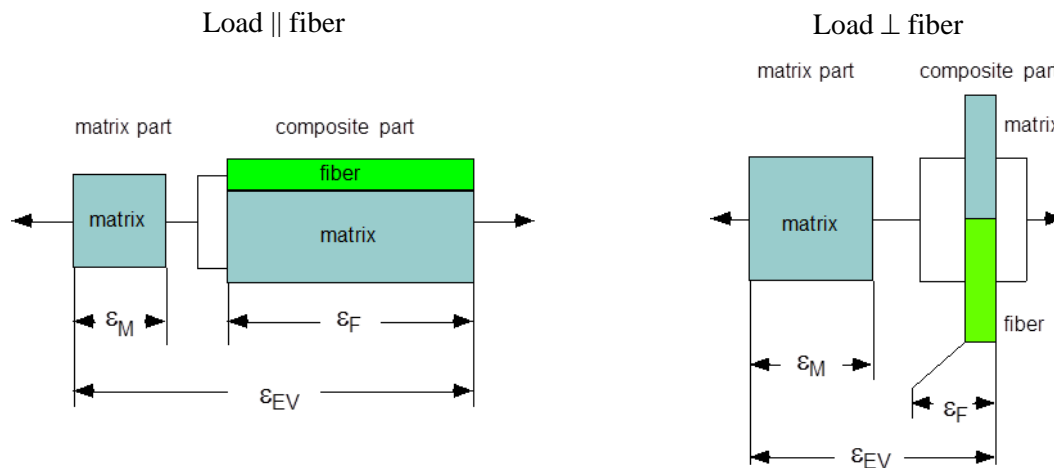


FIGURE 2: Modeling of load states within the Elementary Volume (EV)

For both cases the global strain of the EV ε_{EV} can be expressed in terms of composite strain ε_F and matrix strain ε_M , which all depend on the load given by the initial stress σ_0 . In the case of a creep experiment all strains are time dependent.

$$\text{Load } \parallel \text{ fiber} \quad \varepsilon_{\parallel}(t) = \frac{r}{r+d} \varepsilon_{\parallel,F}(t, \sigma_0) + \frac{d}{r+d} \varepsilon_M(t, \sigma_0) \quad (1)$$

$$\text{Load } \perp \text{ fiber} \quad \varepsilon_{\perp}(t, \sigma_0) = \frac{k}{1+d} \varepsilon_{\perp,F}(t, \sigma_0) + \frac{1+d-k}{1+d} \varepsilon_M(t, \sigma_0) \quad (2)$$

with aspect ratio $r = L/D$, normalized fiber distance $d = a/D$ and efficiency factor k . The efficiency factor k takes into account that the effective fiber cross-section is smaller than $L \cdot D$. For fibers it has the value $k = \sqrt{\pi/4}$. Equation (1) and (2) represent the ultimate strains for a SFRC having a unidirectional fiber orientation. If there is some fiber orientation distribution the measured strain of the SFRC in 1, 2 and 3-direction is determined by both ultimate strains. A first estimation of is done by weighing the ultimate strains with the corresponding orientation factors.

$$\begin{aligned}\varepsilon_1(t) &= f_1 \varepsilon_{\parallel}(t) + f_2 \varepsilon_{\perp}(t) + f_3 \varepsilon_{\perp}(t) \\ \varepsilon_2(t) &= f_1 \varepsilon_{\perp}(t) + f_2 \varepsilon_{\parallel}(t) + f_3 \varepsilon_{\perp}(t) \\ \varepsilon_3(t) &= f_1 \varepsilon_{\perp}(t) + f_2 \varepsilon_{\perp}(t) + f_3 \varepsilon_{\parallel}(t)\end{aligned}\quad (3)$$

2. THEORETICAL CONSIDERATIONS

If one considers the creep behavior of SFRC the strains parallel and perpendicular to the fiber axis, equation (1) and (2), have to depend on time and load given by the initial stress σ_0 . Thus, the creep compliances $S(t)$ are given by

$$\text{Load } \parallel \text{ fiber} \quad S_{\parallel}(t) = \frac{r}{r+d} S_{\parallel,F}(t, \sigma_0) + \frac{d}{r+d} S_M(t, \sigma_0) \quad (4)$$

$$\text{Load } \perp \text{ fiber} \quad S_{\perp}(t, \sigma_0) = \frac{k}{1+d} S_{\perp,F}(t, \sigma_0) + \frac{1+d-k}{1+d} S_M(t, \sigma_0) \quad (5)$$

Assuming purely elastic behavior of the composite part allows for expressing both $S_{\parallel,F}(t)$ and $S_{\perp,F}(t)$ in terms of the reciprocal stiffness of the corresponding composite parts leading to

$$S_{\parallel}(t, \sigma_0) = \frac{r}{r+d} \frac{1}{E_F A_F^{\parallel} + E_M (1 - A_F^{\parallel})} + \frac{d}{r+d} S_M(t, \sigma_0) \quad (6)$$

$$S_{\perp}(t, \sigma_0) = \frac{k}{1+d} \frac{1}{E_F A_F^{\perp} + E_M (1 - A_F^{\perp})} + \frac{1+d-k}{1+d} S_M(t, \sigma_0) \quad (7)$$

The effective fiber cross-sections A_F are given within the EVC by

$$A_F^{\parallel} = \frac{\pi}{4} \frac{1}{(1+d)^2} \quad (8) \quad \text{and} \quad A_F^{\perp} = \frac{k r}{(r+d)(1+d)} \quad (9)$$

Now equations (6) and (7) can be rewritten:

$$S_{\parallel}(t, \sigma_0) = \frac{d}{r+d} S_M(t, \sigma_0) + \frac{r}{r+d} \frac{(1+d)^2}{E_F \frac{\pi}{4} + E_M \left(4(1+d)^2 - \frac{\pi}{4} \right)} \quad (10)$$

$$S_{\perp}(t, \sigma_0) = \frac{1+d-k}{1+d} S_M(t, \sigma_0) + \frac{k}{1+d} \frac{1}{E_F \frac{k r}{(r+d)(1+d)} + E_M \left(1 - \frac{k r}{(r+d)(1+d)} \right)} \quad (11)$$

The creep compliances of a SFRC are completely determined by the creep compliance of the matrix part. This means that the creep behavior of any SFRC can be predicted for any given material combinations, fiber volume contents, fiber orientations and fiber lengths if only the creep compliance of the matrix is known. The mathematical structure of equations (10) and (11) allows for introducing effects of fiber matrix adhesion. Reduced fiber matrix adhesion can be interpreted as a reduction of the

fiber stiffness of the composite part which can be taken into account by an adhesion factor n_{adh} . For long-term creep the adhesion factor should become time dependent as it attributes to e.g. delamination. If the load is applied parallel to the fiber axis the matrix shrinks on the fiber due to the larger Poisson ratio improving adhesion. As mainly tensile stresses in the fiber matrix interface lead to delamination, adhesion effects have only to be taken into account for $S_{\perp}(t, \sigma_0)$. Thus, equation (11) is modified to:

$$S_{\perp}(t, \sigma_0) = \frac{1+d-k}{1+d} S_M(t, \sigma_0) + \frac{k}{1+d} \frac{1}{n_{adh}(t) E_F \frac{k r}{(r+d)(1+d)} + E_M \left(1 - \frac{k r}{(r+d)(1+d)} \right)} \quad (12)$$

The adhesion factor has values between $n_{adh}=0$ (no adhesion) and $n_{adh}=1$ (ideal adhesion).

3. EXPERIMENTAL

3.1 Manufacturing of samples and materials

An injection molding machine Ferromatik Milacron FMF 110 S/2F allowing for both push pull processing (for samples with highly uniform fiber orientation), **Figure 2(left)**, and conventional processing (for samples with the typical skin core fiber orientation) was used to manufacture plates having the dimensions 80x80x2.5mm³. Isotactic polypropylene grades – unreinforced and short fiber reinforced – isotactic polypropylene (iPP), **Table 1**. Tensile test bars were taken out of the plates parallel and perpendicular to the flow direction, **Figure 2(right)**.

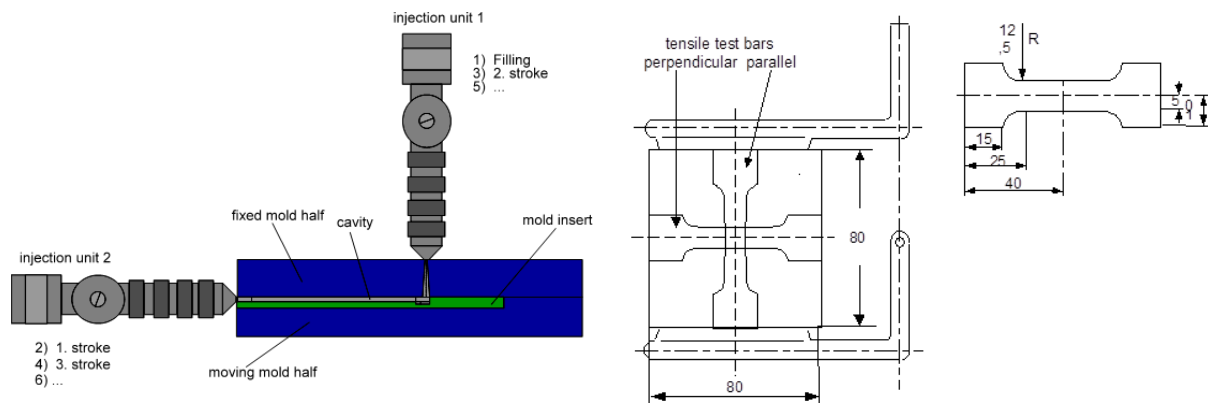


Figure 2: Scheme of push pull processing (**left**) and sample taking and sample geometry (**right**)

Table 1: Investigated polypropylene grades

Material	Trade name	filler content	Comments
PP, unreinforced	Vestolen P7000	0%	unreinforced
PP 30% GF unsized	Vestolen P7052	30%	without coupling agent
PP 30% GF sized	Novolen 1142 PCXGA6	30%	with coupling agent

3.2 Methods

Tensile tests according to ISO 527 were performed with a Zwick 1476 to determine the mechanical anisotropy in terms of initial Young's moduli and strengths.

Creep tests according to ISO 811 were performed with a Zwick 1411 for 2 weeks ($\approx 10^6$ s) at 23°C and 50% humidity. The levels of initial stresses σ_0 were chosen with respect to the yield stress σ_y of

the unreinforced conventionally injection molded PP to 5 MPa, 10 MPa and 15 MPa. This corresponds to approximately 17%, 34% and 50% of σ_y of the PP matrix.

The **fiber orientation** was measured using the sectioning method by evaluating the half axes of the “fiber ellipses” over the cross-section of a sample and expressing the fiber orientation distribution in terms of the 2nd order tensor $\langle a_{ij} \rangle$ [Tucker]. For this evaluation only the main diagonal elements representing the orientation factors are used.

The **fiber length** distribution was determined by pyrolysis of the polymer matrix of a sample piece, spreading the remaining fibers and measuring the length of at least 100 fibers using an image analyzer.

3.3 Evaluation of creep data

The measured creep strain curves $\epsilon(t)$ were evaluated in the following way:

- Transformation to measured creep compliance curves – division by the initial stress σ_0
- Correction of measured creep compliances with respect to Young’s modulus determined by tensile tests [7]
- Calculation of theoretical creep compliance curves using equations (10) and (12) setting $n_{adh} = 1$
- Determination of the adhesion factor n_{adh} by fitting the theoretical creep compliance curves for short times

4. RESULTS AND DISCUSSION

The orientation factors clearly show that push pull processing leads to samples having a significantly higher and more uniform fiber orientation with respect to the flow direction, Table 2. Furthermore, the two short fiber reinforced PP composites differ in their fiber length distribution and mean fiber length, respectively.

Table 2: Orientation factors and mean fiber length (flow direction coincides with f_3)

Material	Orientation factors		Mean fiber length $\langle L \rangle$ μm
	Conventional injection molding	Push pull processing	
PP 30%GF – unsized	$\vec{f}=(0.29, 0.07, 0.64)$	$\vec{f}=(0.16, 0.04, 0.80)$	225
PP 30%GF – sized	$\vec{f}=(0.31, 0.09, 0.60)$	$\vec{f}=(0.11, 0.05, 0.84)$	375

As a consequence this leads to a more pronounced anisotropy of stiffness and strength of push pull processed samples, **Table 3**. The coupling agent in “PP 30%GF – sized” samples leads to a significant increase of the tensile strengths compared to “PP 30%GF – unsized” samples whereas Young’s moduli are not that much affected. This behavior is also partly attributed to the longer fibers in “PP 30%GF – sized” samples. Interestingly, less fiber orientation seems to be beneficial for the overall tensile strengths of “PP 30%GF – sized” samples if processed conventionally. Furthermore, the data show that reinforcement mainly occurs in direction of preferential fiber orientation. In the perpendicular direction the yield stress is often not exceeding the yield stress of the matrix.

Fiber reinforcement reduces in principle the creep and the creep compliance compared to pure matrix creep, **Figure 3**. A more pronounced fiber orientation leads to a further decrease of the creep compliance parallel to the fiber orientation and to an increase perpendicular to the fiber orientation. In

particular, no creep parallel to the fiber orientation was observed for push pull processed samples during the measuring time of 2 weeks. Longer fibers also reduce the creep kinetics perpendicular to the flow direction.

Table 3: Young's moduli and tensile strengths parallel and perpendicular to the flow direction

Material	Processing	E_{\parallel} MPa	$\sigma_{y\parallel}$ MPa	E_{\perp} MPa	$\sigma_{y\perp}$ MPa
PP unreinforced	conventional	1840	28	1740	28
PP unreinforced	push pull	2100	37	1800	32
PP 30%GF – unsized	conventional	4260	32	2780	22
PP 30%GF – unsized	push pull	6030	45	2579	20
PP 30%GF – sized	conventional	5730	80	3570	44
PP 30%GF – sized	push pull	6740	75	2940	27

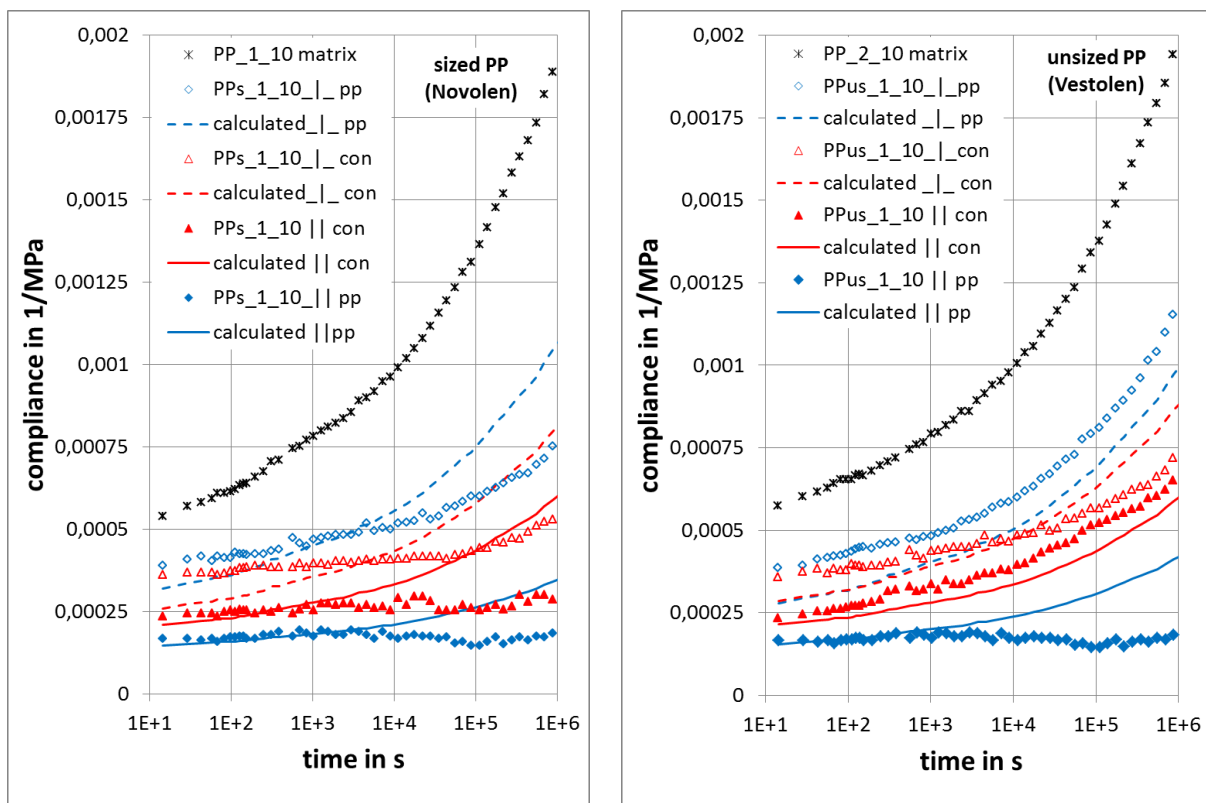


Figure 3: Creep compliances of PP matrix and PP 30GF parallel and perpendicular to the flow direction loaded by an initial stress of 10 MPa; sized Novolen (**left**) and unsized Vestolen (**right**); lines represent creep compliances calculated according to equation (3)

The calculated creep compliances show enhanced creep if compared to the measured data after a certain time. This behavior is related to the corresponding enhanced matrix creep. Obviously fiber reinforcement reduces the creep of the matrix part because of additional internal stress states generated due to fact that fibers hinder the deformation of the composite part. As the matrix part is more strained than the composite part the cross-section of matrix part decreases more than that of the composite part. In principle this means formation of voids what violates the requirement of complete space filling of the EVC. To affirm complete space filling it has be required that the cross-sections of matrix and composites are identical generating boundary forces which reduce the creep of the matrix part.

The predicted creep compliances perpendicular to the fiber orientation are lower than the measured ones for short times. This behavior is more pronounced firstly for the unsized PP Vestolen and secondly for samples having less preferential fiber orientation. The fiber matrix adhesion affects mainly the creep perpendicular to the fiber orientation. Furthermore, the comparison of the creep behavior of sized and unsized PP perpendicular to the fiber orientation shows that enhanced matrix creep occurs later in the case of good fiber matrix adhesion. The deviation of the calculated creep compliance and data for unsized PP is larger than for sized PP allowing for quantifying the fiber matrix adhesion.

Adjusting the adhesion factor n_{adh} of equation (12) for push pull processed samples loaded perpendicular to the fiber orientation within first two time decades yields calculated creep compliances that match much better with data, **Figure 4**. This demonstrates that the basic concept works. The adhesion factor n_{adh} of sized PP was determined to be in the range 0.13 to 0.14 while that of unsized PP was determined to be in the range 0.10 to 0.11. This small value is surprising and unexpected as the yield stresses, Table 3, clearly show the efficiency of the coupling agent.

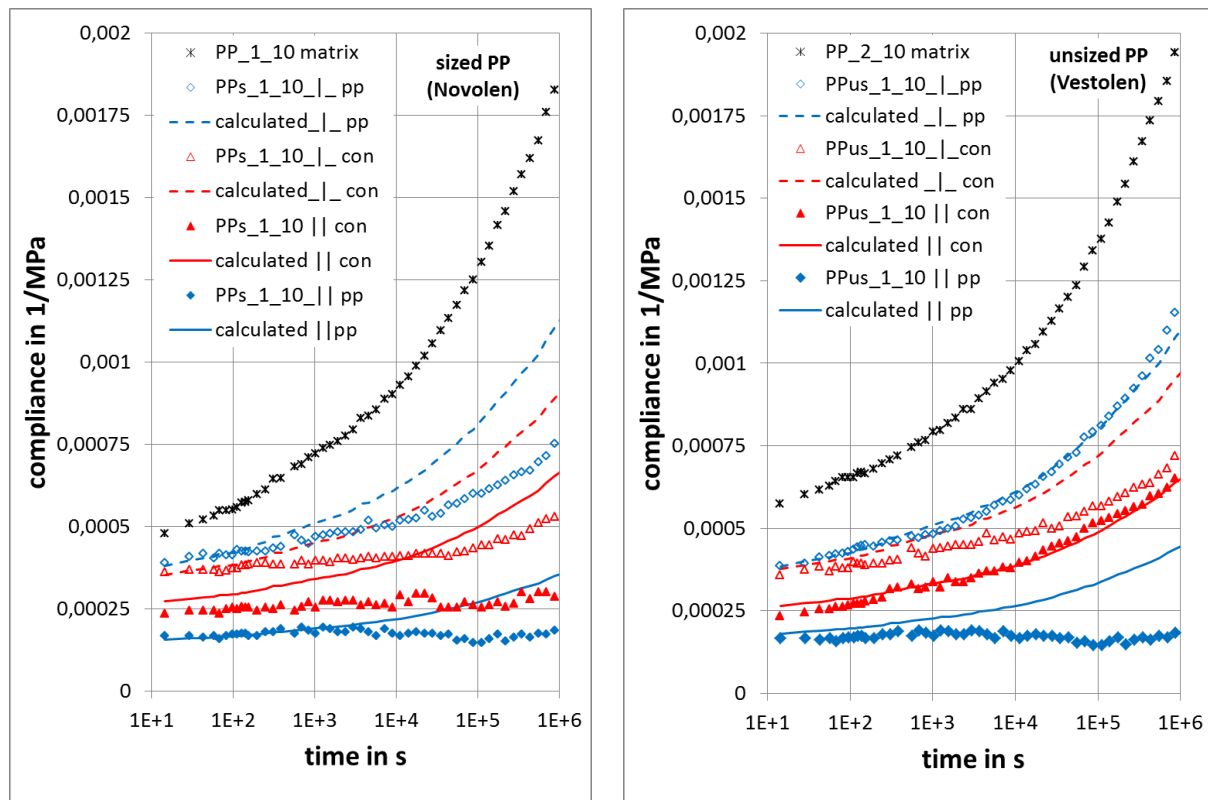


Figure 4: Measured creep compliances of PP 30GF parallel and perpendicular to the flow direction compared to the corresponding calculated creep compliances after adjusting the adhesion factor; sized PP (Novolen) with $n_{adh}=0.13$ (left) and unsized PP (Vestolen) with $n_{adh}=0.11$ (right)

However, the introduction of coupling agent means that one has created a layer around the fiber. If the stiffness of this layer is much smaller than that of the PP matrix the coupling agent does not affect much the creep behavior at the beginning but it prevents debonding of the PP matrix from the fiber surface for significantly longer times.

The equations (3) are a rough estimate to take into account effects of fiber orientation as only the Young's moduli in two directions are known. A more precise approach requires knowing all components of the ultimate stiffness tensor. Only then the transformation of the ultimate stiffness tensor can correctly be performed to generate the properties of the SFRC using the tensor of fiber

orientation. Thus, creep compliances under shear load and POISSON ratios have experimentally to be determined as well as the corresponding models for them.

5. CONCLUSION

In the EVC a SFRC is represented by a single EV consisting of an elastic composite part and a viscoelastic matrix part which determines its ultimate creep behavior. If these ultimate creep properties are transformed with respect to the fiber orientation the creep compliance of SFRC parallel and perpendicular to the flow direction can quantitatively be described. It allows for distinguishing Effects of aspect ratio, fiber orientation and fiber volume content can be distinguished and separately considered. Furthermore, the term describing the compliance of the composite part allows for introducing an adhesion factor to adjust quantitatively the fiber contribution to the composite part. The determined adhesion factors are surprisingly small leading to the questions: i) “Which compliance has the coupling agent in the interface?” and ii) “Does the coupling agent contribute to the creep behavior already at the beginning or only at long times when the yield stress which decreases with time has reached values to affect the creep behavior?”

The comparison between measured data and calculated creep compliances show that the basic concept of the EVC holds but weighing of the ultimate creep properties only with the orientation factors is too rough. This means that experimental data of creep under shear load and measurements of POISSON ratios have to be performed for such highly oriented samples, and the corresponding models have to be derived using the EVC. Furthermore, the creep data show that the introduction of fibers decelerate the creep kinetics of SFRC compared to pure matrix samples. This can be understood in terms of the EVC as matrix part and composite part are coupled. This hinders the reduction of the cross-section of the matrix part leading to a strain dependent compression stress affirming that both matrix part and composite part have identical cross-sections. This means that the real stress acting on the matrix part decreases strain dependently from the initial stress σ_0 to smaller values. Thus, in equation (10) and (12) the matrix compliance $S_M(t, \sigma_0)$ has to be supplemented by a term taking into account this strain dependent stress decrease.

ACKNOWLEDGEMENTS

REFERENCES

- [1] Skourlis TP, Chassapis C, Manoochehri S, The Study on the Optimization of Injection Molding Process Parameters with Gray Relational Analysis, J Reinf Plast Comp, 22, 51-66, 2003 22
- [2] Halpin JC Kardos JL, The Halpin-Tsai-equations: A review, Poly Eng Sci 5, 344-352, 1976
- [3] Tandon GP, Wenig GJ, Average stress in the matrix and effective moduli of randomly oriented composites, Composites Sci Tech 27, 111-132, 1986
- [4] Eshelby JD, The determination of the elastic field of an ellipsoidal inclusion, and related problems, Proc Roy Soc London A241, 376-396, 1957
- [5] Möginger, B, Berechnung mechanischer Kenngrößen von Kurzfaserverbunden mit dem Elementar-Volumen-Konzept, Kautschuk Gummi Kunststoffe 52, 162-169, 1999
- [6] Advani SG, Tucker III CL, The use of tensors to describe and predict fiber orientation in short fiber composites, J Rheo 31, 751-784, 1987
- [7] Möginger B, PhD thesis, appendix B, University of Stuttgart, 1993